LARS Contract Report 120379

Quarterly Progress Report

Evaluation of SLAR and Thematic Mapper MSS Data for Forest Cover Mapping Using Computer-Aided Analysis Techniques

Contract No. NAS 9-15889

Reporting Period: September 1, 1979 - November 30, 1979

Submitted to: Exploratory Investigations Branch
NASA Lyndon B. Johnson Space Center

Prepared by: Laboratory for the Applications of Remote Sensing
Purdue University
West Lafayette, Indiana 47906

Technical Monitor: Dr. D. L. Amsbury
NASA Mail Code SF5
Exploratory Investigations Branch
Houston, Texas 77058

Principal Investigator: Dr. Roger M. Hoffer
Ecosystems Program Leader
LARS/Purdue University
West Lafayette, Indiana 47906

TABLE OF CONTENTS

List of Figures

A. Geometric Adjustment

The evaluation of the spatial characteristics of the data was completed. A program was developed to reduce the spatial distortions resulting from variable viewing distance, and geometrically adjusted data sets were generated.

The objective of the geometric adjustment efforts were: 1) to produce a data set which corresponded geometrically to aerial photography and U.S.G.S. maps of the area, to facilitate identifying training and test areas, and 2) to produce a data set which would provide accurate area estimates from pixel summations. The criteria used in identifying the acceptable level of geometric correction were: 1) consistency of scale in each dimension everywhere in the data set, and 2) equivalency of scale between the two dimensions.

The general features of the routine that was developed for this purpose are:

1) The routine is based on a model which defines the location and dimension of each pixel, for each line in the data set.
2) The model is purely deterministic. There was no attempt made to compensate for stochastic variations in the geometry (i.e., image characteristics resulting from random roll, pitch, yaw, or change in altitude of the aircraft).
3) The data set was truncated at the $\pm 35^{o}$ viewing angle. (See radiometric adjustment for discussion.)
4) No data within the set defined by the bounding viewing angles (i.e., within $\pm 35^{o}$), was omitted.

The along-track scale of the pixel at "nadir" was determined by locating control points on the image and a 1:62,500 U.S.G.S. map, computing the "ground" distance between the points along the component parallel to the flight line (perpendicular to the scan lines), and dividing by the number of scan lines between the two points. The along-track distance per scan line was approximately 7.6 meters. The 2.5 mrad IFOV of the scanner and the 20,000 ft. (6,096 meters) flight altitude would result in a 15.24 meter (50 ft.) scan line width at nadir, which indicates there was an over-scan of approximately 2. A standardized "pixel" dimension of 15.3 x 15.3 meters was chosen due to the spatial characteristics of the data.

The geometric adjustment process is basically a repetitive reassignment of the existing data values to integer multiples of data addresses. The value of the integer multiple expresses the number of "standardized pixels" which will fit into each actual pixel, due to the particular dimensions resulting from its angular displacement from nadir. Figure 1 is a flowchart describing the procedure employed for each channel, for each line of data. The procedure clarifies the fact that data cells in the resulting data set no longer represent pixels on a one-to-one basis. A pixel is now represented by some integer multiple of data cells.

Figure 2 is a Varian image showing the geometric and radiometric characteristics of the original "raw" data set. The vertical line represents the nadir column. Figure 3 was generated from the geometrically adjusted data set.[1/] It should be apparent by comparing Figures 2 and 3, that visually separable units become increasingly compressed in the across-track dimension with increasing distance from the nadir column in the original data set image as compared to the adjusted data set image.

The consistency of scale in each dimension and the equivalency of scale between dimensions (i.e., along-track and across-track) was evaluated by superimposing control points located on a 1:62,500 U.S.G.S. map onto the adjusted imagery using a Zoom Transfer Scope. The coincidence of all control points indicated that the acceptance criterion was met. Geometrically adjusted data sets were then generated for all areas in the study site.

B. Radiometric Adjustment

1) Problem

The potential need for some level of radiometric adjustment was evidenced by an along-track band of high reflectance across different cover types in the Varian imagery. The decision to conduct a radiometric adjustment was based on: 1) classification results are dependent on the amount of variance in reflectance associated with cover type differences; 2) plots of the data and regression analysis employing reflectance levels averaged over lines, by column, by channel, indicated a strong trend with respect to

---

[1/] The images for both Figures 2 and 3 were produced as Varian greyscale printouts of Channel 5 (1.00 - 1.30 μm) data.

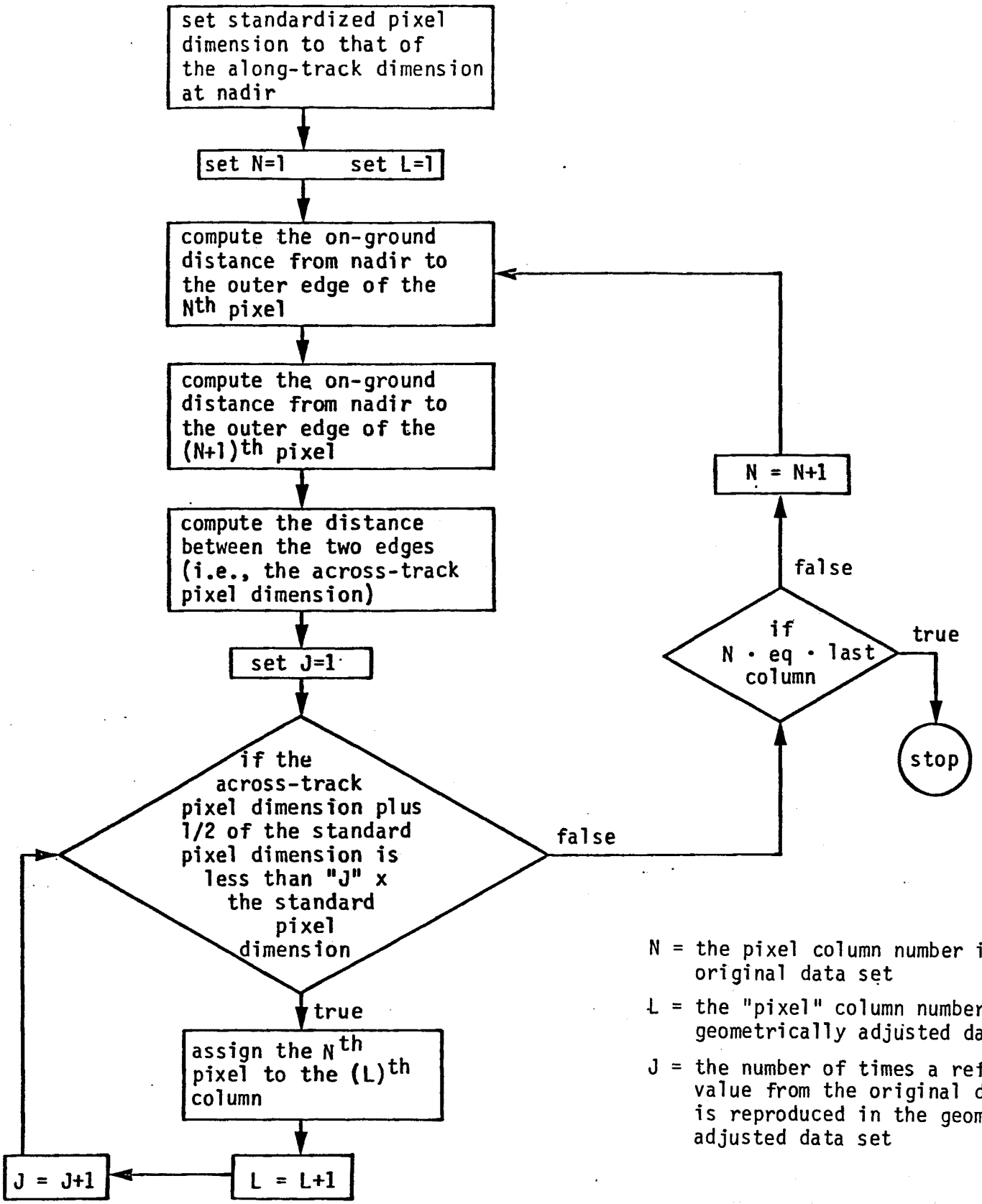

Figure 1. Flowchart of steps taken to geometrically adjust a data set from the NS-001 scanner. This removes, or reduces, differences in pixel widths as a function of changing viewing angles.

Figure 2. Varian imagery of the "raw" data set previous to any manipulations (channel 5, 1.00 - 1.30 μm).

Figure 3. Varian imagery of the geometrically adjusted data set. (channel 5, 1.00 - 1.30 μm)

Fig 3

column (see Figures 4 and 5); and 3) theoretical changes in reflectance associated with changes in viewing angle are considered sufficient to obscure reflectance levels otherwise correlated with cover type.

2) Objective

The objective in radiometrically adjusting the data was to remove or reduce the variance in reflectance extraneous to differences in cover type.

3) Method

Figure 6 provides a summary of the radiometric adjustment method. A multiple regression analysis was employed to explore the viewing angle effect on measured reflectance. Areas in the data set which appeared to have no across-track stratification of covertype were identified. A program was developed which computed the average reflectance by column for each channel, over all of the scan lines in the designated areas. A regression analysis was then run using first, second, and third degree polynomials, for each channel. The regression equations used were:

$$\hat{Y}_{ij} + \beta_{oj} + \beta_{1j}X_1 + \varepsilon_{(ij)}$$

$$\hat{Y}_{ij} = \beta_{oj} + \beta_{1j}X_1 + \beta_{2j}X^2 + \varepsilon_{(ij)}$$

$$\hat{Y}_{ij} = \beta_{oj} + \beta_{1j}X_1 + \beta_{2j}X^2 + \beta_{3j}X^3 + \varepsilon_{(ij)}$$

where:

$\hat{Y}_{ij}$ = predicted reflectance level of the i^{th} column of the j^{th} channel

X = column; 1, ..., 560

X^2 = column squared; $(1)^2$, ..., $(560)^2$

X^3 = column cubed; $(1)^3$, ..., $(560)^3$

β_{oj}, β_{1j}, β_{2j}, β_{3j} are the least squares fitted coefficients of the regression model variables for the j^{th} channel (each beta for each channel is different).

Figure 4. Actual mean and predicted reflectance by column, by channel for channel 1 (0.42 - 0.52 μm) and channel 4 (0.76 - 0.90 μm).

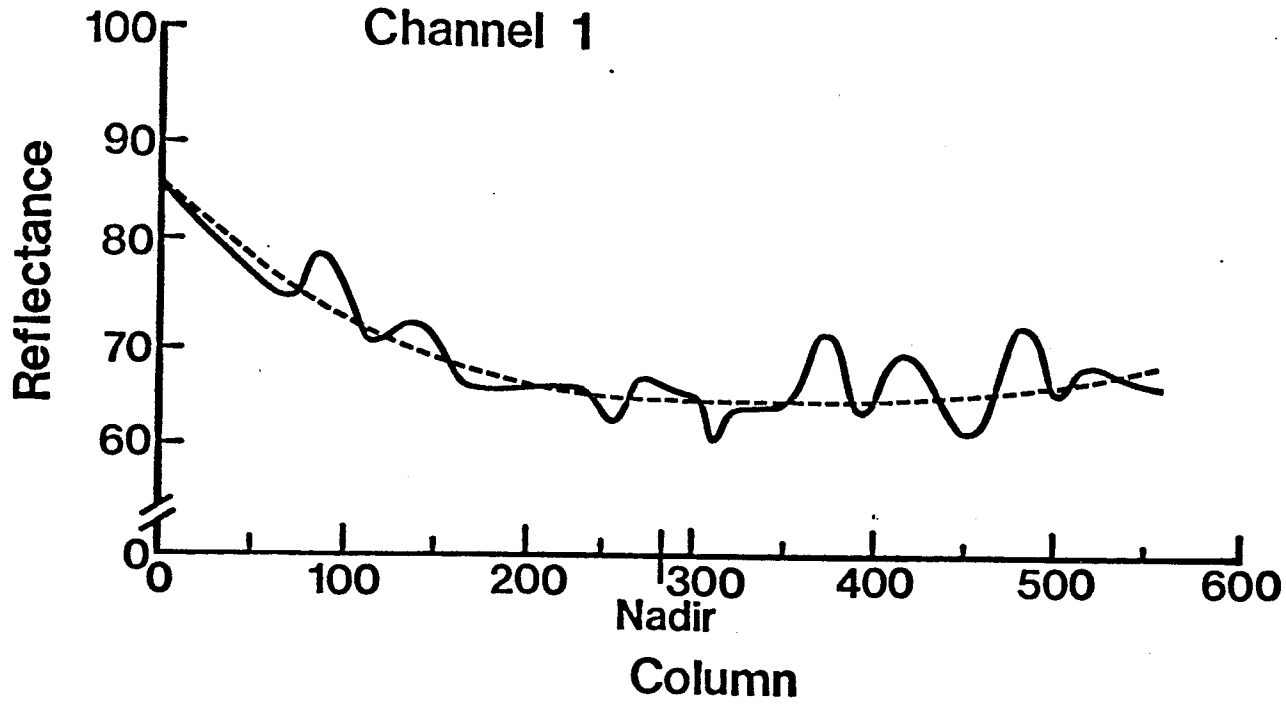
Channel 1
Reflectance
100
90
80
70
60
0
0
100
200
300
400
500
600
Nadir
Column

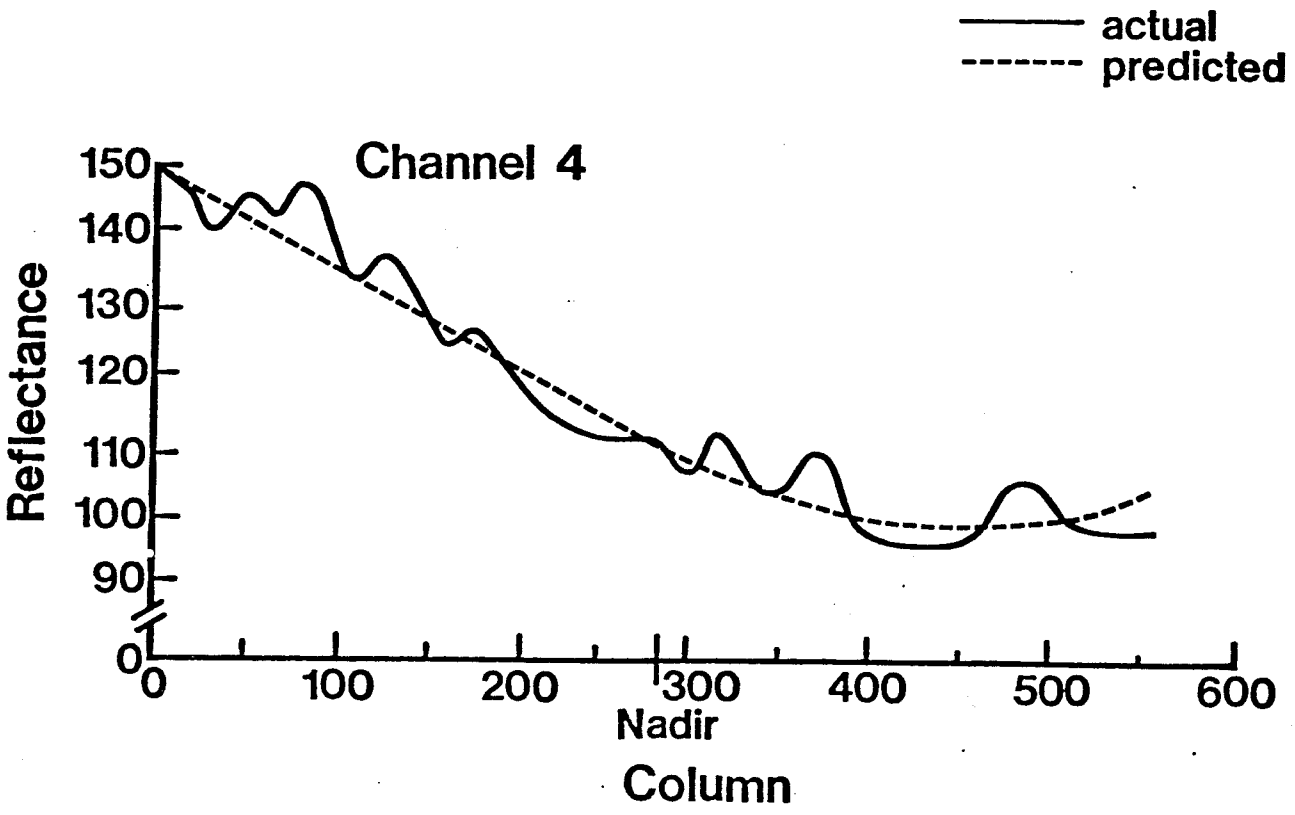
actual
predicted
Channel 4
Reflectance
150
140
130
120
110
100
90
0
0
100
200
300
400
500
600
Nadir
Column

Figure 5. Actual mean and predicted reflectance by column, by channel for channel 6 (1.55 - 1.75 μm) and channel "7" (10.4 - 12.50 μm).

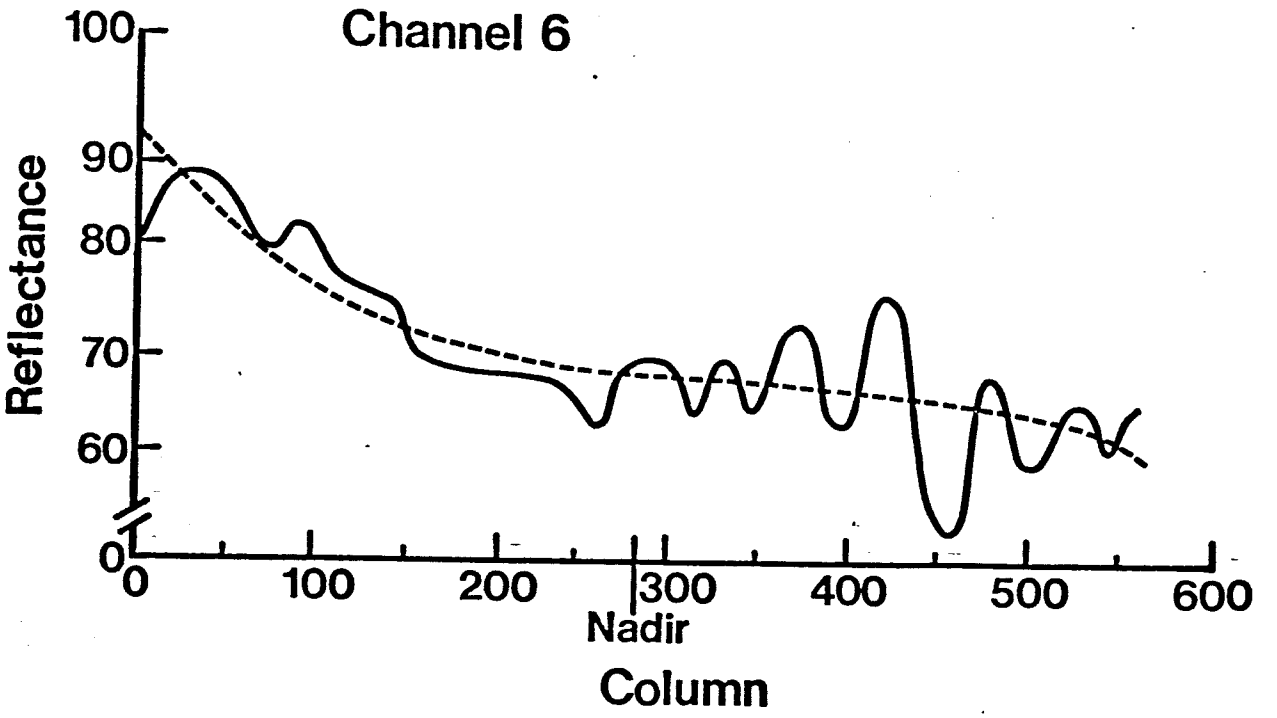
Channel 6
Reflectance
100
90
80
70
60
0
0
100
200
300
400
500
600
Nadir
Column


actual
predicted

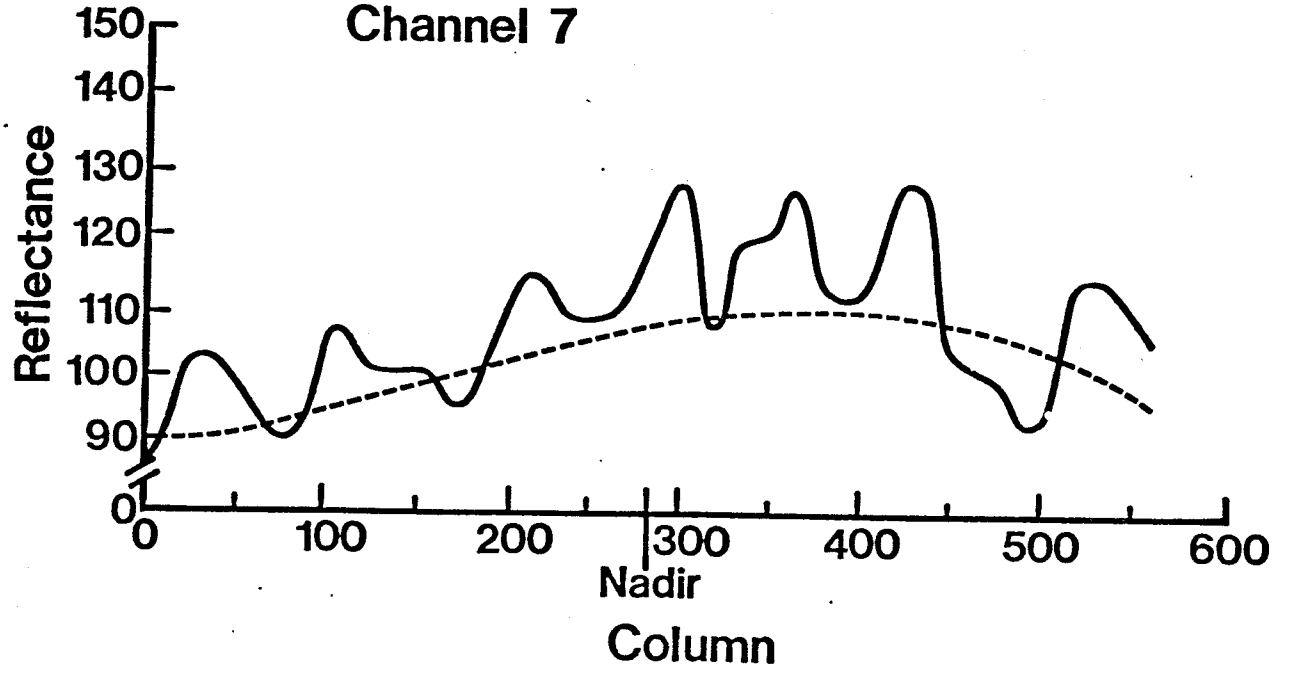
Channel 7
Reflectance
150
140
130
120
110
100
90
0
0
100
200
300
400
500
600
Nadir
Column

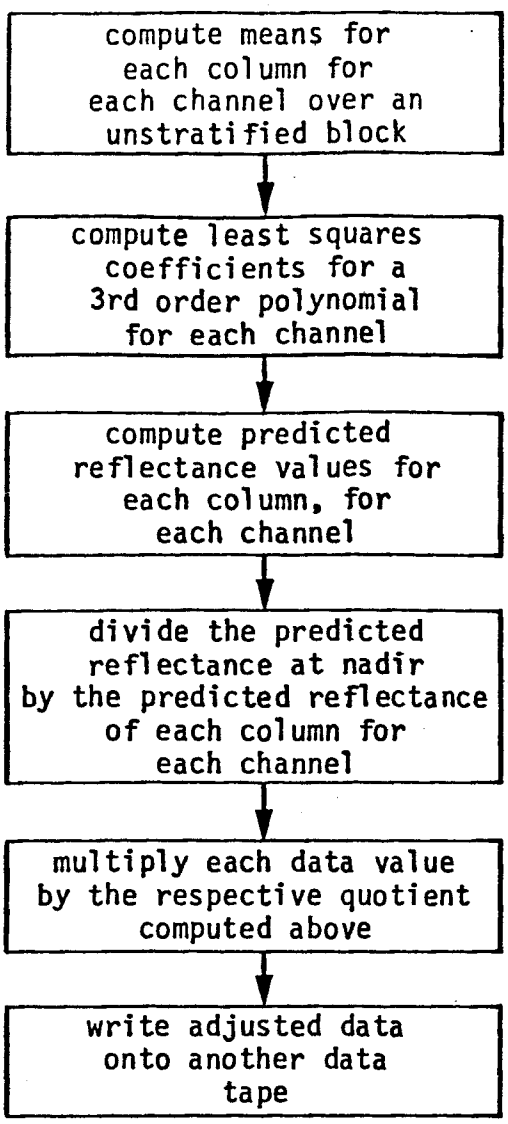

Figure 6. Flowchart of steps taken to radiometrically adjust an aircraft scanner data set in an attempt to remove radiometric variance associated with viewing angle.

If the areas from which the data were taken to conduct the analysis had cover types randomly distributed over the area such that each column had a nearly equivalent fraction composed of each cover type, then the averaging of reflectance over all lines in each column would remove the variance assocated with cover type, and any variance in reflectance between columns should be a function of column or some covariant (e.g., viewing angle). The areas were, by visual inspection, unstratified and were considered to provide a sufficient approximation to the above condition such that the amount of variance accounted for by the regression model is the expected variance due to viewing angle over an assumed constant cover type.

Prior to actually conducting a radiometric adjustment of the data, the potential components of this source of variance were examined to provide information regarding the expected shape of this prediction function. The major components of this source of variation are thought to be: 1) an interaction between cover type and viewing angle with respect to solar angle, and 2) "atmospheric effects." The interaction between cover type and viewing angle results in changes in measured reflectance due to changes in the total area illuminated versus area in shadow within the pixel (Anuta, 1973). The area in illumination is at a maximum when the reflecting surface is viewed along the path of incoming radiation (i.e., when the viewing angle is coincident with the zenith solar angle). As the viewing angle is gradually reduced (i.e., shifting the viewing orientation toward nadir), the relative area in illumination versus shadow decreases and measured reflectance, therefore, decreases. The rate of this change approaches zero near nadir. However, as the viewing angle is increased (i.e., shifting the viewing orientation upward, or away from coincidence with the solar zenith angle), the relative area in illumination versus shadow does not change, since areas in shadow will continue to lie beyond the reflecting object from the point of view of the observer. With regards to this consideration, the actual mean reflectance by column appears consistent with theory.

This relationship (between mean reflectance by column, and column location with respect to nadir) is an interaction effect with cover types, in that the change in relative area in illumination versus shadow is dependent on a vertically nonequivalent distribution of the actual reflecting surfaces. This component of the viewing angle effect is less for vertically

equivalent reflecting surfaces such as bare soil than for vertically non-equivalent surfaces as are found in forested or otherwise vegetated cover types. While this variability involves cover type differences, it results in greater variance in reflectance within particular cover types when the azimuthal solar angle is zero, and therefore needs to be removed or reduced.

It is of interest to note that this change in reflectance with viewing angle and solar angle is directly proportional to the cosine of the azimuthal angle (i.e., the angle separating the plane of propagation from the plane of observation). Figure 7 displays this relationship and schematically defines the terms. This within cover type source of variance is therefore greatest when Ψ equals zero (i.e., the planes are coincident) and smallest when Ψ equals 90^{o}. Since the verical heterogeneity of the reflecting surface differs for different cover types, this source of variance may actually assist in classification efforts when the plane of observation is separated from the plane of propagation by an angle of 90 degrees. While this area is in need of attention, it is beyond the scope of the current study.

Figure 8 is a Varian greyscale representing channel 5 of the geometrically adjusted, radiometrically unadjusted data set. Figure 9 is a Varian image of the geometrically and radiometrically adjusted data set (channel 5). Visual inspection of the two images should make apparent the reduction in across-track (or by column) variation in reflectance in the adjusted data set as compared to the unadjusted data set.

The second component of the viewing angle source of variance is primarily an "atmospheric effect." The following discussion is greatly simplified, as its inclusion here is only to provide the rationale for radiometrically adjusting the data set and using the particular model that was developed.

Radiant energy passing through a segment of the atmosphere has a probability of colliding with atmospheric constituents dependent on the density of the gas molecules and larger suspended particles in the segment considered (Kondratyev 1969, Jurica 1973). Collision with atmospheric constituents results in either scattering or absorption.

Absorption is fairly invariant due to changes in viewing angle with respect to solar angle, except for the small increase in the probability of

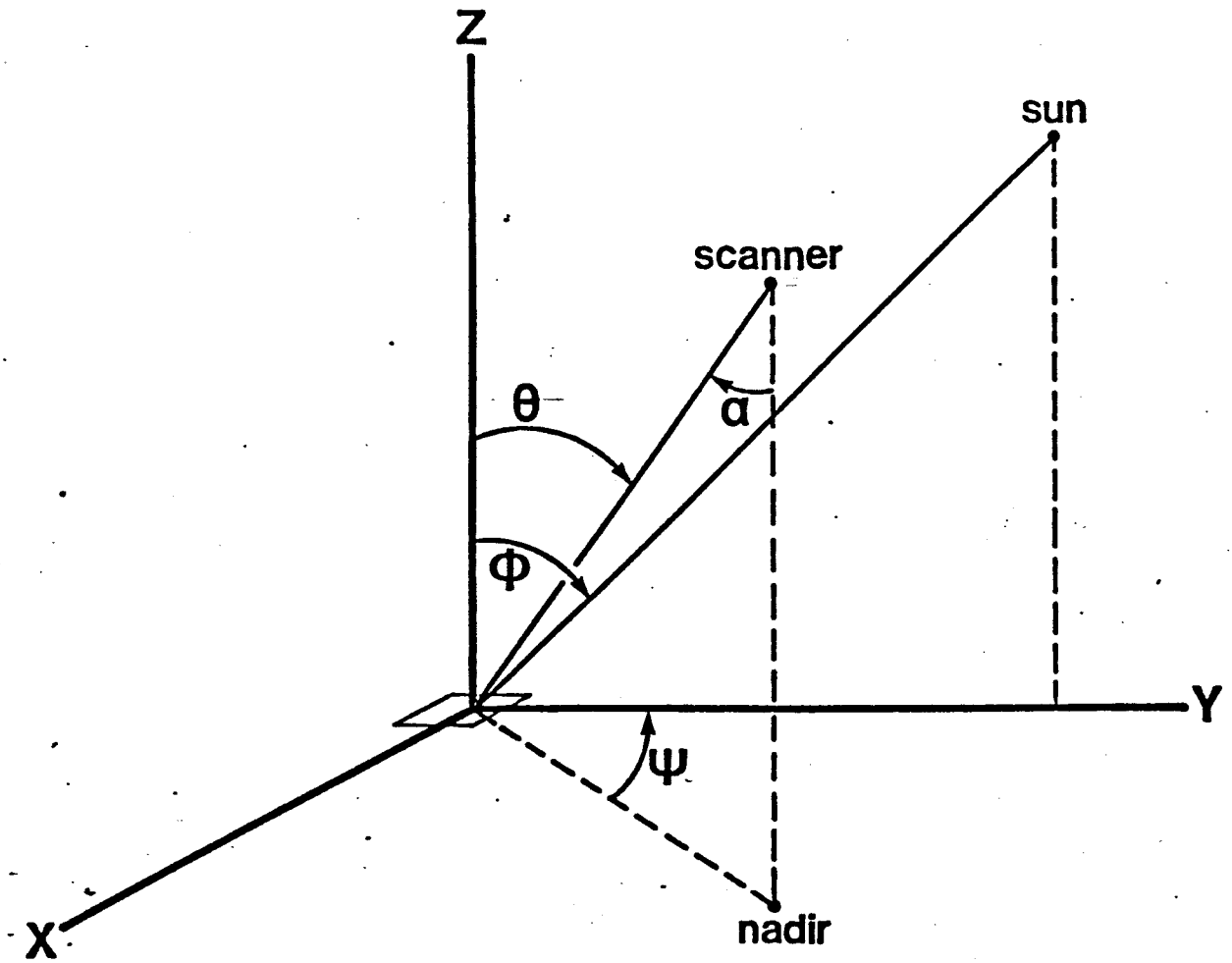

Figure 7. Schematic of the angular relationships between the illumination source (sun) and the location of the scanner. An arbitrary pixel is centered at the origin. The zenith solar angle is represented by Φ, the viewing angle is represented by α, and the azimuthal solar angle, the angle between the plane of propagation (defined by the sun, the origin, and the y-axis) and the plane of observation (defined by the scanner, nadir, and the origin), is represented by Ψ. The zenith viewing angle is represented by Θ.

Figure 8. Varian imagery of the geometrically adjusted, radiometrically unadjusted data set (channel 5).

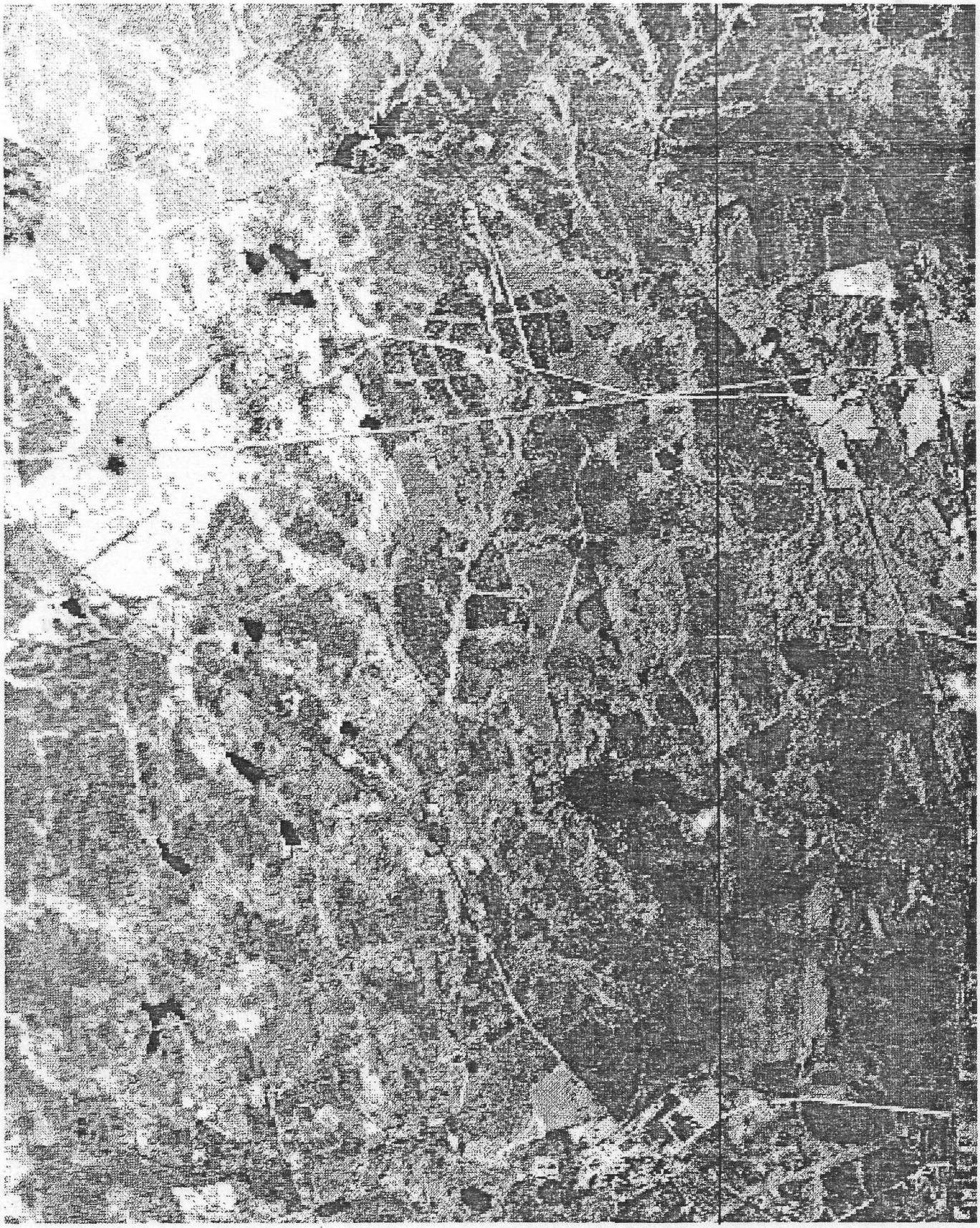

Figure 9. Varian imagery of the geometrically, radiometrically adjusted data set (channel 5).

absorption due to the increased optical thickness of larger viewing angles. This is considered negligible.

Scattering, however, is highly direction-dependent. For both Rayleigh and Mie scattering, the principle component of the scattered light is along the axis of transmission. Rayleigh type scattering, "molecular" scattering of primarily visible light, has equal backward and forward components approximately twice that of the sideward components (Kondratyev, 1969). Figure 10 is an illustration of the relative distribution of scattered light for all potential directions. Mie scattering is very similar except the forward scattering is predominant over backward scattering, which is dominant over lateral or side scattering (Jurica, 1973).

These relationships result in greater amounts of light being scattered into the transmission path than away from this path. Hence, when viewing is along the transmission path measured radiance is greater relative to that of other viewing angles with respect to the solar angle due to the greater additive effect of forward and backward scatter.

This would suggest a dampened cosine function centered on the column corresponding to the angle of viewing coincident with zenith solar angle.

In the context of the above considerations, the model was considered appropriate. Existing LARSYS software was then modified to produce the radiometrically adjusted data sets. This basically involved inserting code which computed a normalizing multiplier for each column, for each channel. Data values from each line in each channel were then multiplied by the respective normalizing multiplier for each particular column. The product was then read onto tape in MIST format. The normalizing multiplier is the quotient of the predicted reflectance at nadir and the predicted reflectance for each column.

$$NM_{ij} = \frac{\hat{Y}_{in}}{\hat{Y}_{ij}}$$

where:

NM_{ij} = the normalization multiplier of the j^{th} column of the i^{th} channel.

$\hat{Y}_{in}$ = predicted reflectance at nadir of the i^{th} channel.

$\hat{Y}_{ij}$ = predicted reflectance of the j^{th} column of the i^{th} channel.

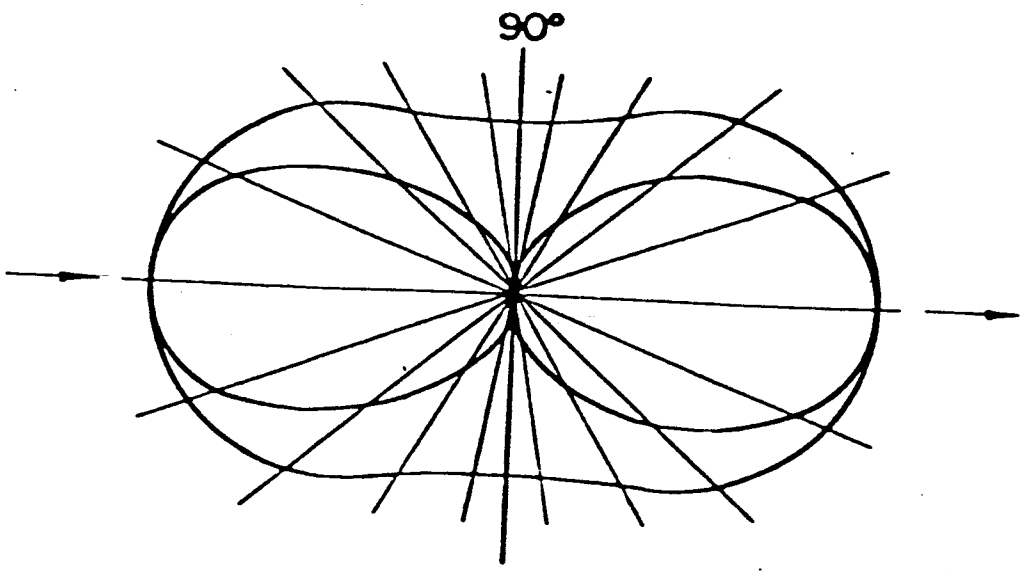

Figure 10. Schematic of the Rayleigh Scattering probability density function, indicating the probabilities of scattering a photon in any of all possible directions, given the direction of incidence. The horizontal axis is the axis of incidence.

C. Software Development for Spatial Resolution Degradation

Software is currently being developed for the degradation of the spatial resolution of the geometrically and radiometrically adjusted data set (here-after referred to as the "adjusted" data set). This is expected to be completed early in the forthcoming quarter.

D. Completion of the Cover Type Maps

The cover type maps have been completed. The maps will also provide a qualitative index for comparison of classification results.

E. Training and Test Field Selection

Training and test field selection has been initiated and is expected to be completed during the next quarter. Training sets will be provided by a combination of multicluster blocks (Fleming, 1977) and selected training fields. Test fields will be defined as 4 x 5 "pixel" blocks such that they will provide test statistics for the 57 x 79 meter resolution of the Landsat data. The statistical sampling design for locating the test fields is currently being defined.

F. SAR Data Acquisition

Neither of the two RB-57 missions initially requested were flown during the 1979 growing season, and consequently, the radar data was not obtained. Therefore, all activities involving use of the SAR data will have to be delayed until 1980.

SAR data from SEASAT was provided by NASA/JSC as a substitute, but examination of the imagery representing the contents of the tape indicated that the study area was not included on the data set provided. Mr. C. A. Anderson of Goodyear Aerospace Corporation was then contacted by LARS concerning acquisition of the needed SAR data. A computer scan of the field imagery indicated that imagery including the study area was available only for 1971. This imagery was not requested since the eight-year difference in dates rendered it unsuitable for the research objectives.

G. Landsat Data Acquisition

The May 13, 1979 overpass of Landsat II (Scene ID 21572-15120) has been backlogged for correction of problems apparently resulting from the

scanline pulse problems experienced during that period. Several telephone calls to Robert Fienberg's office at GSFC have been made in an attempt (unsuccessful thus far) to prompt the processing and transmittal to EDC of this data tape. It is hoped that this Landsat data will be received during the forthcoming quarter.

H. Planning and Support of the Fall Missions

Information concerning the fall NC-130/NS-001 and RB-57/APQ-102 SLAR missions was provided the mission manager. Communications were maintained to monitor the status of the missions at the time they were to be flown. However, due to aircraft scheduling problems and equipment malfunctions, neither mission was flown.

I. Site Visit

The study area was visited by R. Latty and B. Goodrick to identify areas not identifiable on the aerial photography. The visit was made during the period October 18-22. A survey was made of crop conditions, soil moisture levels, stage of senescence of both deciduous forest areas and herbaceous cover on behalf of the anticipated fall mission. The visit also provided an opportunity for B. Goodrick, the senior analyst, to become familiar with the cover types occurring in the area.

II. PROBLEMS ENCOUNTERED

Two major problems encountered during this quarter were:

1) Neither the RB-57/APQ-102 nor the NC-130/NS-001 fall missions were flown. Failure to execute these missions as planned has resulted in a total lack of radar data and has, thereby, precluded work on a major component of this project.

2) As previously stated, there has been an inordinate delay in the processing of the required Landsat II data at Goddard Space Flight Center. This has precluded all preprocessing activities for Landsat data planned for this quarter. Every effort is being made to prompt the handling and transmittal of the May 13, 1979 data tape.

III. PERSONNEL STATUS

The following personnel committed the respective percentages of time to the project during this past quarter:

Name	Position	Ave. Monthly Effort (%)
Anuta, Paul	Reformatting/Preprocessing	10
Crosley, Rodney	Research Assistant	67
Hoffer, Roger	Principal Investigator	37
Kline, Nancy	Secretary	3
Latty, Richard	Research Associate	50
Peterson, John	Associate Director	3
Prather, Brenda	Secretary	25

IV. ANTICIPATED ACCOMPLISHMENTS

The following are the anticipated accomplishments of the forthcoming quarter (December 1, 1979 - February 29, 1980):

1) Completion of the spatial resolution degradation software.
2) Completion of the training and test field selection.
3) Begin classification analyses.

The advancement made in the analysis sequence (i.e., comparing the classification results of the different spatial resolutions) will depend on the time required to complete the writing of the resolution degradation software. It is believed that this will be completed early in the forthcoming quarter.

REFERENCES CITED

Anuta, P.E. and D.F. Strahorn (1973) "Sun Angle Effect Preprocessing with Predicted Ramp Functions." LARS Technical Memorandum T-12 050673.

Jurica, G.M. and M.L. Murray (1973) "The Atmospheric Effect in Remote Sensing of Earth Surface Reflectivities." LARS Information Note 110273.

Kondratyev, K. YA. (1969) Radiation in the Atmosphere. Academic Press, 912 pp.

RELATED REFERENCES

Fleagle, R.G. and J.A. Businger (1963) Atmospheric Physics. Academic Press, 334 pp.

Jurica, G.M. (1973) "Atmospheric Effects on Radiation Measurements." LARS Information Note 011573.

_____, and C.L. Parsons (1974) "Atmospheric Correction of Remotely Sensed Spacecraft Data." LARS Information Note 032974.

Turner, R.E. (1975) "Atmospheric Effects in Multispectral Remote Sensor Data." Final Report, NASA, Johnson Space Center, Earth Observations Division, Contract # NAS 9-14123, Task VIII.